Intercomparison of Nocturnal Lower-Atmospheric Structure Observed with Lidar and Sodar Techniques at Pune, India

P. C. S. DEVARA, P. ERNEST RAJ, B. S. MURTHY, G. PANDITHURAI, S. SHARMA, AND K. G. VERNEKAR

Indian Institute of Tropical Meteorology, Pune, India

(Manuscript received 7 March 1994, in final form 13 October 1994)

ABSTRACT

Coordinated experiments to study the nocturnal lower atmosphere were conducted on selected nights during April–August 1991 using an argon ion lidar and a Doppler sodar at the Indian Institute of Tropical Meteorology, Pune (18°32′N, 73°51′E, 559 m MSL), India. The lidar and the sodar have been operated simultaneously so as to detect the nocturnal atmospheric structure in the common air volume sampled by both the techniques. By analyzing the thermal and aerosol structures in the vertical profiles of the sodar and the lidar signal intensity, the nocturnal mixed-layer height or ground-based inversion height and the stably stratified or multiple elevated layers aloft have been determined. The top of the nocturnal ground-based inversion observed in the sodar records is taken as the height above the ground where the negative vertical gradient in aerosol concentration first reaches a maximum in the lidar records. The results of the study indicate an agreement between the lidar-derived mixing depth and the sodar-derived heights of the ground-based inversion and the low-level wind maximum.

1. Introduction

Active remote sensors such as the lidar, the sodar, and the radar can scan large volumes of the atmosphere in a much shorter time than possible with in situ measurements. For this reason, many research topics of current interest would benefit greatly from the availability of remote sensors capable of monitoring the state of the atmosphere continuously in time and over extended areas. By using different remote sensors, either collectively or individually, some researchers have studied the evolution of the planetary boundary layer (PBL), which plays an important role in the natural as well as human-induced atmospheric processes (e.g., Browning et al. 1973). While exhaustive information has been obtained from these studies regarding the daytime convective boundary layer (CBL), fewer studies are available on the evolution of the nighttime boundary layer (NBL). The NBL evolves due to the radiative cooling of the surface and of the air over the surface of the earth, and varies with time from sunset to sunrise in response to changing surface conditions.

The nocturnal mixed layer is generally known to vary strongly with time—growing, collapsing, and then growing again, several times over the course of the night. Measurement of the NBL height is feasible with the observations of turbulence, a parameter that is limited in the NBL compared to that in the CBL. Application of the instruments operating on different principles is a very good means to determine these heights. However, for the purposes of parameterization of the NBL, various convenient ways have been adopted by different investigators to define this important layer (Hanna 1969; Melgarejo and Deardorff 1974; Blackadar 1976; André and Mahrt 1982).

Though many diagnostic models (Wyngaard 1975; Nieuwstadt 1984) and parameterization schemes (Rao and Snodgrass 1979) have been developed, observational studies of the nocturnal lower atmosphere, of which the boundary layer is a part, are sparse (Mahrt et al. 1979; Li et al. 1983). Nevertheless, some researchers have made attempts to study the nocturnal mixed-layer height from the lidar, the sodar, and the meteorological observations (Derr and Little 1970; Wycoff et al. 1973; Russell et al. 1974; Coulter 1979; André 1983; Beyrich and Weill 1993). The present state of our understanding of the nocturnal boundary layer depth has been reviewed by several investigators in different contexts (Brown and Hall 1978; Koracin and Berkowicz 1988; Singal 1989).

Joint observational experiments to study the nocturnal lower atmosphere over a tropical urban station have been conducted during the clear night sky conditions on 24 April, 1 and 30 May, and 19 June 1991 at the Indian Institute of Tropical Meteorology (IITM), Pune, India. To study the time evolution of the nighttime mixed layer over the typical terrain of the observational site the experiment has also been conducted from the early-night through the early-morning hours of 1–2 August 1991. In these experiments, a bistatic,

Corresponding author address: Dr. P. C. S. Devara, Indian Institute of Tropical Meteorology, Pune 411 008, India.

continuous wave, argon ion lidar and a monostatic, pulsed, Doppler sodar have been operated simultaneously to view the same or closely neighboring atmospheric volumes. In this paper we present the details of the lidar and the sodar employed in the experiment, the terrain of the experimental site, and the methodology used for determining the nocturnal atmospheric structure from the lidar and the sodar signatures. Also, we discuss here the results obtained from the individual experiments as well as from the intercomparison of the structure and dynamics of the nocturnal lower atmosphere as revealed by both remote sensing devices from the through-out-night experiment conducted on 1–2 August 1991.

2. Instrumentation and methodology

The lidar and the sodar deployed for the experiment are located approximately 200 m apart (in the north–south plane) in the institute's campus. Table 1 summarizes the systems' parameters.

TABLE 1. Main characteristics of lidar and sodar used in the experiment.

	Lidar	Sodar
Mode of operation	Bistatic	Monostatic
Transmitter		
Energy source	Argon ion laser	Electromechanical transducer
Wavelength	514.5 nm	0.22 m
Pulse width	Continuous wave	200 ms
Power	200 mW	100 W (peak)
Pulse repetition rate	—	6.4 min^{-1}
Beamwidth	0.6 mrad	210 mrad
Antenna	Reflecting mirror	1.8-m-diameter collocated parabolic dish
Receiver		
Beamwidth	0.5–6.5 mrad	210 mrad
Antenna	25-cm-diameter Newtonian reflector	Same as transmitter
Predetection filter passband width	1.0 nm	150 Hz
Detector	Peltier-cooled RCA C31034A photomultiplier	Same as transmitter energy source

a. *The lidar system*

The potential application of the lidar technique for remote sensing of aerosol distributions in the PBL has been well documented by several investigators (Collis et al. 1964; Zuev 1982; Sasano et al. 1980; Devara 1989; Hashmonay et al. 1991). These studies have also helped to document the structure and the stratification of the atmospheric boundary layer by using aerosol inhomogeneities as tracers. The aerosols that are lifted due to daytime convective activity would be suspended for a considerable amount of time in the lowest layers of the atmosphere and those generated particularly near the surface would confine to lower levels during the nighttime. During the night, the aerosol layers are horizontally stratified because mixing is limited by the surface radiation inversions. The nighttime radiative cooling of the surface and of the air over the surface of the earth induces stable stratification near the ground or sometimes far above the nocturnal mixed layer, and advection and/or subsidence begins to play a role in determining the aerosol concentration aloft. As suggested by Lenschow et al. (1979), the terrain variations lead to significant local variations in the thermal and the dynamical forcings that can influence the patterns that are formed due to the surface-generated aerosols particularly during the early morning transition from a stable to a convective boundary layer.

The lidar used in the present experiment has been in regular operation at the institute since 1986 for remote sensing of the atmospheric aerosols and the trace gases in altitudes from 20 m to 5.5 km. It consists of a Lexel 95-4 model, tunable (at discrete steps) argon ion laser as transmitter and a 25-cm-diameter, f/7.6 Newtonian telescope as receiver equipped with an optics assembly composed of condensing–collimating lenses, narrowband interference filter (1 nm FWHM), and Peltier-cooled PMT. The lidar has been operated in the bistatic mode with its transmitter horizontally separated from the receiver by 60 m. The vertically sent laser beam was scanned by the receiver at preselected elevation angles corresponding to different altitudes. The scattered signal strength profiles thus collected have been converted into the aerosol number density profiles using the inversion method described elsewhere (Devara and Raj 1987; Raj and Devara 1989).

Since the lidars, through light scattering, detect the aerosol distribution itself within the atmospheric structure, and changes in backscatter with time and space yield information on transport and diffusion processes, they are very useful for determining the height to which pollution originating in the mixed layer has been carried. One way of determining these heights from the lidar-derived aerosol concentration profiles is through the computation of the normalized concentration gradients (NCG) as suggested initially by Endlich et al. (1979) and Sasano et al. (1982) and later used extensively by the authors for the study of the urban aerosol layer structure over Pune (Devara and Raj 1990, 1991; Raj and Devara 1993). The NCGs were computed from the aerosol number density gradients normalized by the local aerosol number density using the following formula suggested by Sasano et al. (1982):

$$\mathrm{NCG}(Z_i) = 100\left[\frac{\Delta C_i}{\Delta Z_i C(Z_i)}\right],$$

where $\Delta C_i = C(Z_{i+1}) - C(Z_{i-1})$ and $\Delta Z_i = Z_{i+1} - Z_{i-1}$. The normalization procedure followed here

eliminates the absolute calibration of the lidar system, and also the local variations in the aerosol concentration. The NCG profiles thus constructed have been used to study the nocturnal structure of the lower atmosphere. The largest negative gradient nearest to the surface in the lidar backscatter (or the aerosol number density) is associated with the sharpest decline from high to low particulate concentrations and thus marks the mixing depth (Endlich et al. 1979). This method of marking the mixing depth has been widely used to study the evolution of the daytime mixed layer, which extends, most of the time, beyond 1 km. The nighttime mixed-layer heights extending up to 1500 m during the postsunset period in fine weather have also been reported by some researchers (Sasano et al. 1983). The positive gradients often occur above the mixing depth and they denote the aerosol layer structures associated with the stable conditions.

b. *The sodar system*

In recent years, the sodar technique has been widely used in the studies of the planetary boundary layer structure and of the mesoscale meteorological phenomena associated with different types of terrains (Lenschow et al. 1979; Neff 1988; Surridge and Goldreich 1988). The sodars are found to be particularly useful for continuous monitoring of the thickness of the shallow stable regions that form during the nighttime and hence they are useful devices for air quality studies (Holzworth 1967). These devices measure thermal turbulence when used in the backscatter (or the monostatic) mode and are sensitive to both the temperature and the wind velocity fluctuations when used in the forward-scatter (or the bistatic) mode. In either mode, the received acoustic power may be determined by small-scale temperature structure or thermal turbulence in the sampled volume. The monostatic sodar sounding vertically measures the height of the turbulent nocturnal boundary layer.

The sodar used in the experiment was installed at the institute in 1989. It is a three-axis, monostatic, pulse Doppler sodar manufactured by M/S AeroVironment Inc. It operates at an acoustic frequency of 1.5 kHz and comprises three parabolic antennas, of which two ($\pm 30°$ off the zenith in the east–west and the north–south directions) are used for the determination of the horizontal wind components and the third is sensitive to the vertical wind component of the backscattered echo. The system is capable of making measurements of wind speeds, directions, and characteristics of inversion and thermal structures in the altitudes between 50 and 1500 m. Output consists of the profiles of total wind speed ($m\ s^{-1}$) and direction ($°$), vertical wind ($m\ s^{-1}$), and the return signal strength (in arbitrary units) at desired interval of time. This interval can be set according to the experimental requirements. The sodar was operated concurrently with the lidar, and its averaging periods (about 10 min) were synchronized with those used for the lidar observations.

c. *Topography of the experimental site*

The detailed description of the topography of the experimental site can be found in our earlier publications (Devara and Raj 1990). However, the main features of the terrain and the human activities around the observational site are presented here. The site is located at an elevation of about 570 m MSL and is surrounded by the hillocks having elevations as high as 760 m MSL, the majority with elevation greater than 610 m MSL. The stone quarries (east side) and brick kilns (west side) situated about 1 km from the site are the local anthropogenic sources influencing the observations (particularly in the lowest layers of the atmosphere) of the lidar and the sodar. In addition, there is major urban activity to the east of the site; to the west is a sparsely populated area. The terrain is believed to induce complex wind fields with marked horizontal and vertical variability in wind speed, direction, and turbulence. The environment in the immediate vicinity of the station is urban.

d. *Observations and analysis*

Both the lidar and the sodar have been operated continuously from 1900 to 0530 LST 1–2 August 1991, and the vertical distributions of the scattered intensity measured over every 30-min period were analyzed. The time–height variations of the strength of the lidar and the sodar echo returns, which contain the aerosol and the temperature fine-scale structures, respectively, are used to study the structure and the dynamics of the nocturnal lower atmosphere. The mean wind field as well as the individual wind components derived from the Doppler frequency spectra of the sodar and their time–height variations are also used to study the low-level wind (jet) variations, which normally are associated with the nocturnal temperature inversions and turbulence. The surface-level temperature, relative humidity, wind speed, and wind direction data were obtained from the meteorological sensors installed at the experimental site.

3. Discussion of results

a. *Nocturnal atmospheric structure and its time evolution*

The nocturnal boundary layer is generally stably stratified and is formed during the clear nights over the land. It begins to establish soon after the sunset, continues to persist until the early morning, and dissipates after the sunrise when the thermal convection develops near the surface. Radiative cooling, shear-generated turbulence, and horizontal advection are responsible for the evolution of the NBL, whereas the

low-level winds may modify the structure of the NBL. The variation of the NBL height is dependent on the shear stress distribution within the layer and, thus, mixing height is usually taken to be the depth of the shallow turbulent region adjacent to the ground. The term, mixing depth or mixed-layer height, derived from the aerosol vertical distribution, is used in this paper in place of the expression "ground-based inversion height" or "ground-based shear layer" (Singal 1989) during nighttime. This usage may not always be valid in view of the association between relative humidity and particulate concentration observed by the lidar (MacKinnon 1969). However, the top of the ground-based inversion can be taken as the mixing height during the nighttime if the height of the largest negative concentration gradient close to the ground is the same as the top of the temperature inversion obtained from the radiosonde data (Tomback and Chan 1976; Russell and Uthe 1978a,b).

b. *Inference from lidar observations*

Figure 1 shows the lidar profiles of the NCG derived from the aerosol vertical distributions obtained at 30-min intervals on the night intervening 1–2 August 1991. As explained in section 2a, the largest negative gradient close to the ground marks the mixing depth and the regions with prominent positive gradients aloft denote stably stratified layers. During the postsunset period over this station, mixing depths have been found to be as low as 160 m and lie around 550 m, while the stable layers appear around 750 m (Raj and Devara 1993). The mixing depth and the stable layer heights inferred from each profile of the NCG are presented in Table 2. Mixing depths varied from 160 to 360 m (average depth being 273.7 m) with a minimum occurring around midnight. Stable layers form up to an altitude of 880 m.

c. *Inference from sodar observations*

The backscattered intensity gradients at different altitudes have been computed from the half-hourly measured sodar return echo signal distributions and are shown in Fig. 2. Information from these gradients together with the criterion supplied by the sodar manufacturers (Technical Manual—Doppler sodar model-2000, M/S AeroVironment, California) were used for inferring the heights of the ground-based inversion and elevated layers. The heights of the mixed layer and the stably stratified layers determined from the lidar observations are compared with those of the ground-based

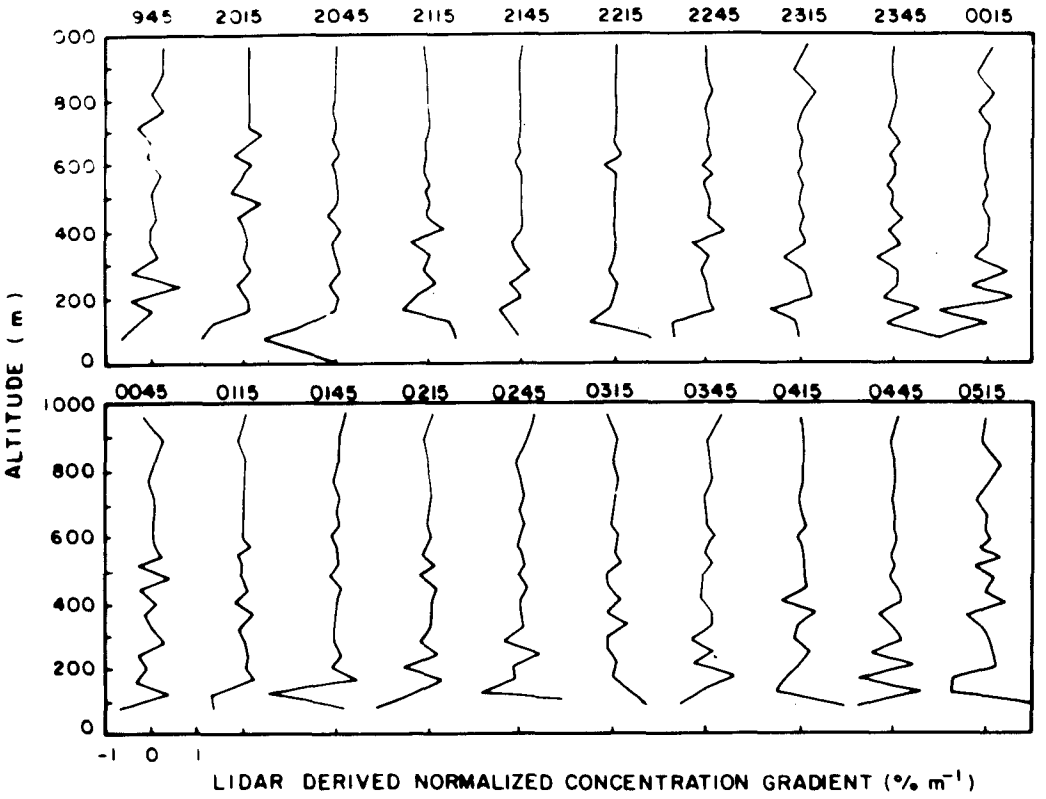

FIG. 1. Normalized concentration gradient (NCG) profiles corresponding to aerosol number density profiles obtained with the lidar on 1–2 August 1991.

TABLE 2. Nocturnal mixed-layer and stable-layer heights as observed by lidar and sodar techniques on 1–2 August 1991.

Time (LST)	Mixed-layer height (m)		Stable-layer height (m)	
	Lidar	Sodar	Lidar	Sodar
2000–2030	240	345	360, 480, 670	735
2030–2100	240	315	400, 630	525, 585
2100–2130	360	345	400, 710	705
2130–2200	360	345	400	615, 675, 765
2200–2230	280	345	630	705
2230–2300	280	255	565, 630, 815	675, 915
2300–2330	320	255	360, 820	705, 770, 885
2330–0000	320	265	360, 440, 670	855, 975
0000–0030	240	215	710, 820	885
0030–0100	160	165	480, 880	795
0100–0130	320	195	360, 565	945
0130–0200	200	230	440, 510	450, 540
0230–0300	280	225	440, 510	495
0300–0330	280	375	510, 595, 760	—
0400–0430	280	285	360, 440, 625	—
0430–0500	240	285	400, 595	—

inversion and the multiple elevated layers inferred from the sodar observations in Table 2.

Figure 3 shows the time sequence of the vertical profiles of the horizontal wind field observed with the sodar on the night of 1–2 August 1991. The distinct occurrence of the nocturnal low-level wind maximum and its changes are evident from the figure. The low-level wind maximum (or jet) generally appears above the nocturnal temperature inversion (Jury and Tosen 1987). As suggested by Blackadar (1957), the elevation of the low-level jet in each profile can be considered as the height of the ground-based inversion, which is consistent with those deduced from the lidar and the sodar scattered intensity profiles.

d. Comparison between lidar- and sodar-derived mixed- and stable-layer heights

The time variations of the mixing depths inferred from the observations obtained by simultaneous operation of the lidar and the sodar are shown in Fig. 4. Their agreement is good. Except during the late evening hours, the lidar- and the sodar-derived depths agreed within ±50 m throughout the observation period. Note the minimum depth inferred from the observations around midnight and a phase difference of about 90 min between the lidar- and sodar-derived depths. The larger differences between the depths observed

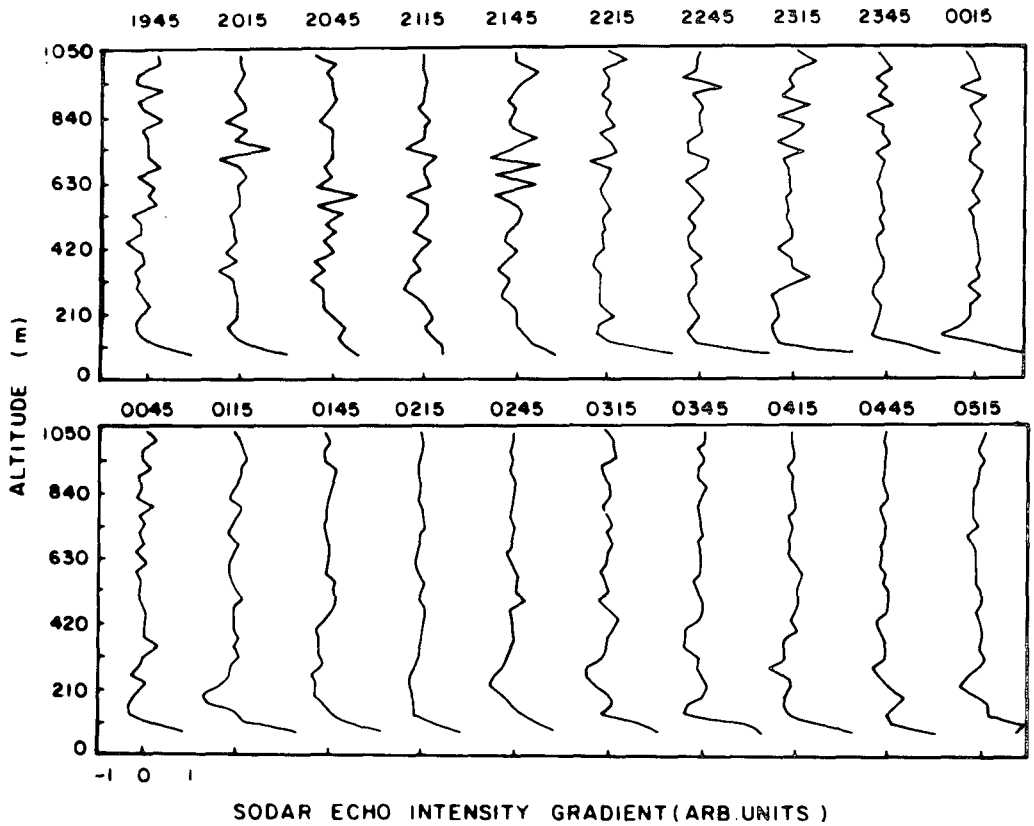

FIG. 2. Backscatter echo intensity gradient profiles obtained with the sodar on 1–2 August 1991.

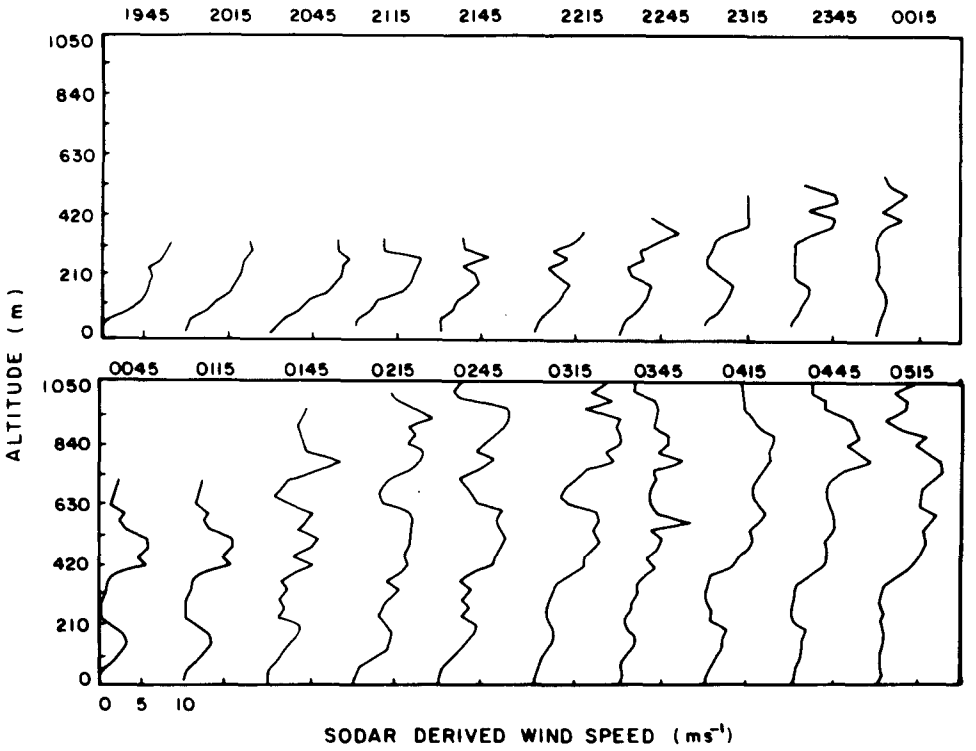

FIG. 3. Space–time variations in the wind field derived from the Doppler sodar signatures obtained every 30 min on 1–2 August 1991. Nocturnal occurrence of the low-level wind maximum can be noted.

by both the instruments during the postsunset period may be due to the differences in the atmospheric processes responsible for the lidar and the sodar returns as explained by Russell et al. (1974).

Since the meteorological parameters are known to influence the aerosol characteristics and the temperature structure function, the observations of surface-level temperature, relative humidity, wind speed, and wind direction have been collected simultaneously at the experimental site and are also shown in Fig. 4. Considering the local effects due to surrounding human activities and the experimental terrain, the shifting wind flows are believed to create sudden changes in the aerosol structures aloft and the advected air carrying differing aerosol content leads to changes in the temperature structure function. The varying direction in association with the magnitude of wind may result in sharp changes in both the aerosol and the temperature structures (Sasano et al. 1980; Maughan et al. 1982). The larger differences observed between the mixed-layer heights determined by the lidar and the sodar around 2000, 0100, and 0400 LST are considered to be due to such effects. It may be noted that the minimum winds correspond to the minimum height of the mixed layer around midnight.

e. Determination of urban air pollution potential from lidar and sodar observations

The mixing depth limits the vertical transport of pollutants. The rate at which these pollutants are transported can be determined from ventilation coefficient, that is, the product of the mixing depth and the mean wind speed through the mixed layer. The higher the ventilation coefficient, the more the atmosphere is able to dispose the pollutants and, thus, these coefficients provide an index of air pollution potential. Typical values are less than 6000 $m^2 s^{-1}$ in the afternoon and less than 2000 $m^2 s^{-1}$ in the morning (Gross 1970).

Figure 5 shows the temporal variation of the ventilation coefficients computed using the lidar- and the sodar-derived mixing depths and the mean wind speed through the mixed layer observed by the sodar on 1–2 August 1991. The maximum coefficient is found to be around 2500 $m^2 s^{-1}$, while the minimum is around 130 $m^2 s^{-1}$. The low ventilation coefficients observed on a typical night during the southwest (SW) monsoon season (June–September) in the present study could be mainly due to the lower mixing depths (Raj and Devara 1992). The aerosol pollutant concentrations are minimal over this station during the SW monsoon season, and the pollutants are captured by cloud and precipitation elements (Devara et al. 1994). Hence, the observed low ventilation coefficients in the present

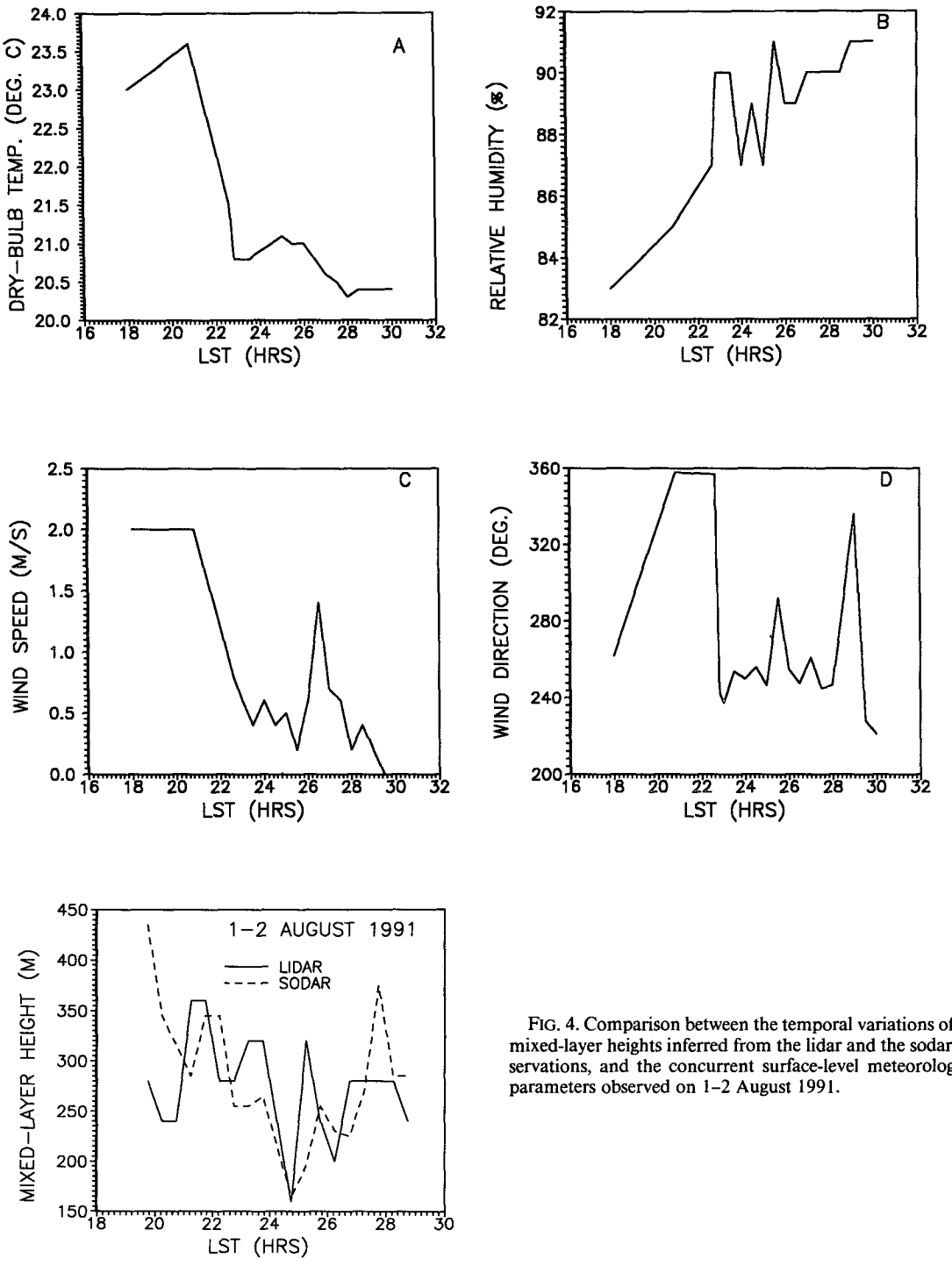

FIG. 4. Comparison between the temporal variations of the mixed-layer heights inferred from the lidar and the sodar observations, and the concurrent surface-level meteorological parameters observed on 1–2 August 1991.

study conducted during the month of August may not be truly indicative of any air pollution potential.

4. Summary and conclusions

The results of the study of the nighttime atmospheric structure observed simultaneously with the lidar and the sodar at a tropical urban station at Pune, India, have been presented. The nocturnal mixed-layer heights documented by the lidar and the sodar showed a good agreement (±50 m) and exhibited a phase difference of about 90 min. The average nocturnal mixing depths determined from the lidar and the sodar observations have been found to be consistent with those

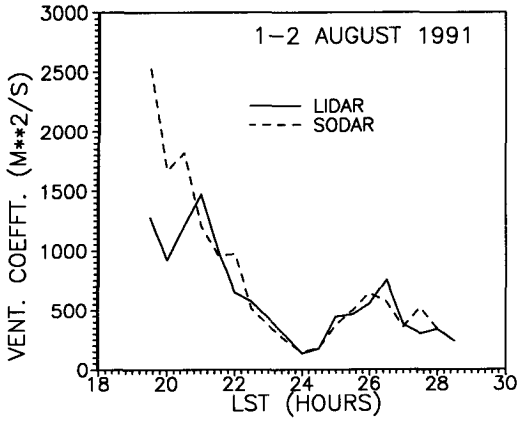

FIG. 5. Nocturnal variation of the ventilation coefficient inferred from the lidar and the sodar observations.

estimated from the Doppler sodar–derived wind profile observations. The temporal variations in the height of the mixed layer and the associated ventilation coefficients exhibited a minimum around midnight and this corresponds to minimum wind speed during that time. In conclusion, considering the role of the experimental terrain in the evolution of the ground-based inversion and multiple stable layers in the nocturnal lower atmosphere, the results of the present coordinated experiment are promising. One important application of the collocated lidar–sodar pair could be the study of the transport and the diffusion of pollutants across the elevated temperature inversions by making detailed and quantitative comparison of the lidar and the sodar data. This will be the subject of further work.

Acknowledgments. Authors are grateful to Prof. R. N. Keshavamurty, Director IITM, and Dr. A. S. R. Murty for their encouragement and support. The financial support of the Department of Science and Technology, Government of India, for the procurement of Doppler sodar is acknowledged. The authors are grateful to the reviewers for their constructive comments and suggestions, which helped to improve the original manuscript.

REFERENCES

André, J. C., 1983: On the variability of the nocturnal boundary layer depth. *J. Atmos. Sci.*, **40,** 2309–2311.

——, and L. Mahrt, 1982: The nocturnal surface inversion and influence of clear air radiative cooling. *J. Atmos. Sci.*, **39,** 864–878.

Beyrich, F., and A. Weill, 1993: Some aspects of determining the stable boundary layer depth from sodar data. *Bound.-Layer Meteor.*, **63,** 97–116.

Blackadar, A. K., 1957: Boundary layer wind maxima and their significance for the growth of nocturnal inversion. *Bull. Amer. Meteor. Soc.*, **38,** 283–290.

——, 1976: Modelling the nocturnal boundary layer. Preprints, *Third Symp. on Atmospheric Turbulence, Diffusion and Air Quality,* Raleigh, NC, Amer. Meteor. Soc., 46–49.

Brown, E. H., and F. F. Hall Jr., 1978: Advances in atmospheric acoustics. *Rev. Geophys. Space Phys.*, 47–110.

Browning, K. A., D. Beran, M. J. S. Quigley, and C. G. Little, 1973: Capabilities of radar, sodar and lidar for measuring the structure and motion of the stably stratified atmosphere. *Bound.-Layer Meteor.*, **5,** 195–200.

Collis, R. T. H., F. G. Fernald, and M. G. H. Lidga, 1964: Laser radar echoes from a stratified clear atmosphere. *Nature,* **203,** 1274–1275.

Coulter, R. L., 1979: A comparison of three methods for measuring mixed-layer height. *J. Appl. Meteor.*, **18,** 1495–1499.

Derr, V. E., and C. G. Little, 1970: A comparison of remote sensing of the clear atmosphere by optical, radio and acoustic radar techniques. *Appl. Opt.*, **9,** 1976–1992.

Devara, P. C. S., 1989: Active remote sensing of the atmosphere using lasers. *J. Sci. Indust. Res.*, **48,** 71–83.

——, and P. E. Raj, 1987: A bistatic lidar for aerosol studies. *IETE Tech. Rev.*, **4,** 412–415.

——, and ——, 1990: Lidar monitoring of urban aerosol layer structure. *Indian J. Environ. Protection,* **10,** 907–913.

——, and ——, 1991: Study of atmospheric aerosols in a terrain-induced nocturnal boundary layer using bistatic lidar. *Atmos. Environ.*, **25A,** 655–660.

——, ——, and S. Sharma, 1994: Remote sensing of atmospheric aerosol in the nocturnal boundary layer using lidar. *Environ. Pollut.*, **85,** 97–102.

Endlich, T. M., F. L. Ludwig, and E. E. Uthe, 1979: An automatic method for determining the mixing depth from lidar observations. *Atmos. Environ.*, **13,** 1051–1056.

Gross, E., 1970: The National Air Pollution Potential Forecast Program. ESSA Tech. Memo. WBTM NMC 47, U.S. Dept. of Commerce, 28 pp.

Hanna, S. R., 1969: The thickness of the planetary boundary layer. *Atmos. Environ.*, **3,** 519–536.

Hashmonay, R., A. Cohen, and U. Dayan, 1991: Lidar observations of atmospheric boundary layer in Jerusalem. *J. Appl. Meteor.*, **30,** 1228–1236.

Holzworth, G. C., 1967: Mixing depths, wind speeds and pollution potential for selected locations in the USA. *J. Appl. Meteor.*, **6,** 1034–1044.

Jury, M., and G. R. Tosen, 1987: The winter nocturnal layer jet over eastern Transval. A case study sequence. *SA J. Sci.*, **83,** 228–233.

Koracin, D., and R. Berkowicz, 1988: Nocturnal boundary layer height: Observations by acoustic sounders and predictions in terms of surface layer parameters. *Bound.-Layer Meteor.*, **43,** 65–83.

Lenschow, D. H., B. B. Stankov, and L. Mahrt, 1979: The rapid morning boundary-layer transition. *J. Atmos. Sci.*, **36,** 2108–2124.

Li Xing-Seng, J. E., J. E. Gaynor, and J. C. Kaimal, 1983: A study of multiple stable layers in the nocturnal lower atmosphere. *Bound.-Layer Meteor.*, **26,** 157–168.

MacKinnon, D. J., 1969: The effect of hygroscopic particles on the backscattered power from a laser beam. *J. Atmos. Sci.*, **26,** 500–510.

Mahrt, L., R. C. Heald, D. H. Lenschow, and B. B. Stankov, 1979: An observational study of the structure of the nocturnal boundary layer. *Bound.-Layer Meteor.*, **17,** 247–264.

Maughan, R. A., A. M. Spanton, and M. L. Williams, 1982: An analysis of the frequency distribution of sodar derived mixing heights classified by atmospheric stability. *Atmos. Environ.*, **16,** 1209–1218.

Melgarejo, J. W., and J. W. Deardorff, 1974: Stability functions for the boundary-layer resistance laws based upon observed boundary-layer heights. *J. Atmos. Sci.*, **31,** 1324–1333.

Neff, D. D., 1988: Observations of complex terrain flows using acoustic sounders: Echo interpretation. *Bound.-Layer Meteor.*, **42,** 207–228.

Nieuwstadt, F. T. M., 1984: Some aspects of the turbulent stable boundary layer. *Bound.-Layer Meteor.*, **30,** 31–35.

Raj, P. E., and P. C. S. Devara, 1989: Some results of lidar aerosol measurements and their relationship with meteorological parameters. *Atmos. Environ.*, **23,** 831–838.

——, and ——, 1992: Laser radar application to air pollution potential measurements during post-sunset period. *J. Optics,* **21,** 87–92.

——, and ——, 1993: On the stable stratification of the nocturnal lower troposphere inferred from lidar observations over Pune, India. *Bound.-Layer Meteor.*, **65,** 197–205.

Rao, K. S., and H. F. Snodgross, 1979: Some parameterizations of the nocturnal boundary layer. *Bound.-Layer Meteor.*, **17,** 15–28.

Russell, P. B., and E. E. Uthe, 1978a: Regional patterns of mixing depth and stability: Sodar network measurements for input to air quality models. *Bull. Amer. Meteor. Soc.*, **59,** 1275–1287.

——, and ——, 1978b: Acoustic and direct measurements of atmospheric mixing at three sites during an air pollution incident. *Atmos. Environ.*, **12,** 1061–1074.

——, ——, and F. L. Ludwig, 1974: A comparison of atmospheric structure as observed with monostatic acoustic sounder and lidar techniques. *J. Geophys. Res.*, **79,** 5555–5566.

Sasano, Y., H. Shimizu, N. Sugimoto, I. Matsui, N. Takeuchi, and M. Okuda, 1980: Diurnal variation of the atmospheric planetary boundary layer observed by a computer-controlled laser radar. *J. Meteor. Soc. Japan,* **58,** 143–148.

——, A. Shigematsu, H. Shimizu, N. Takeuchi, and M. Okuda, 1982: On the relationship between the aerosol layer height and mixed layer height determined by laser radar and low-level radiosonde observations. *J. Meteor. Soc. Japan,* **60,** 889–895.

——, I. Matsui, H. Shimizu, and N. Takeuchi, 1983: Automatic determination of atmospheric mixed layer height in routine measurements by a laser radar. *J. Japan Soc. Air Pollut.*, **18,** 175–183.

Singal, S. P., 1989: Acoustic sounding stability studies. *Encyclopedia of Environmental Control Technology,* P. N. Cheremisinoff, Ed., Gulf Publishing Co., 1003–1061.

Surridge, A. D., and Y. Goldrich, 1988: On the spatial characteristics of the nocturnal stable boundary layer over a complex urban terrain. *Atmos. Environ.*, **22,** 1–6.

Tombach, I., and M. Chan, 1976: Estimation of mixing depth and inversion height by acoustic radar—A comparison with in situ measurements. *Proc. 17th Conf. on Radar Meteorology,* Seattle, WA, Amer. Meteor. Soc., 313–320.

Wycoff, R. J., D. W. Beran, and F. F. Hall Jr., 1973: A comparison of the low level radiosonde and the acoustic echo sounder for monitoring atmospheric stability. *J. Appl. Meteor.*, **12,** 1196–1204.

Wyngaard, J. C., 1975: Modelling the planetary boundary layer-extention to the stable case. *Bound.-Layer Meteor.*, **9,** 441–460.

Zuev, V. E., 1982: *Laser Beams in the Atmosphere.* Plenum, 347–464.